AIAA JOURNAL
Vol. 36, No. 2, February 1998

Use of Linearized Euler Equations for Supersonic Jet Noise Prediction

R. R. Mankbadi,* R. Hixon,† S.-H. Shih,‡ and L. A. Povinelli§
NASA Lewis Research Center, Cleveland, Ohio 44135

The use of linearized Euler equations for direct prediction of supersonic jet noise is explored. It is shown that a high-order numerical scheme coupled with proper boundary treatment can produce a stable solution nearly free from reflections. Results are verified against analytical results for sound radiated by instability waves. Applicability of this approach to real jets is explored by taking the inflow disturbances to be random in time and comparing the computed sound field to the experimentally measured one.

Nomenclature

D = jet exit nozzle diameter
e = total energy per unit volume
M_e = jet exit Mach number
p = pressure
U_e = jet exit velocity
u = axial velocity
v = radial velocity
w = azimuthal velocity
ρ = density
ρ_e = jet exit density

I. Introduction

THE compressible Navier–Stokes equations govern the process of sound generation and propagation to the far field for a real jet flow. However, current computer capabilities make accurate direct numerical simulation (DNS) of high-Reynolds-number turbulent jets impractical. Therefore, an extension of the large eddy simulation (LES) approach for the prediction of sound generation and propagation was proposed.[1,2] In this approach, the Navier–Stokes equations are spatially filtered into large-scale components, which are calculated directly, and small-scale components, which are modeled. In a LES, the noise generated by the small-scale components is not captured; however, it is known that the large-scale structures are more efficient than the small ones at radiating noise.[3–7] The LES approach has been used successfully to predict the noise radiated by a supersonic jet, but it is still a CPU-intensive approach, especially for three-dimensional calculations.

The present work explores the use of the less computationally demanding linearized Euler equations (LEEs) for supersonic jet noise predictions. The LEE approach neglects both viscosity and nonlinear effects. The viscous effects may not be important because the large-scale dynamics in free shear flows essentially are inviscid.[8] Nonlinearity seems to be important in subsonic jets[9]; however, it is not clear how important the nonlinear effects are for supersonic jets.

Several analytical investigators[5,6,10–17] have studied the physics of jet noise based on the stability-wave equations. In such analytical models, the sound source is represented by an instability wave assuming a normal mode decomposition for the disturbances. Upon substituting these assumptions into the LEEs and neglecting nonparallel flow effects, the stability-wave equations are obtained. These equations are used to describe the sound source in the jet. From this, the radiated sound field then can be computed using acoustic analogy or matched asymptotic expansion. Various degrees of success have been achieved with this approach.

LEEs are more general than the stability-wave equations in several regards. Because LEEs do not require the normal mode decomposition, they simultaneously describe both the sound generation and the propagation. Thus, the problems of matching the near-field sound source to the far-field radiated sound are avoided. LEEs also can allow for sound generation by other modes besides the stability modes. Furthermore, because it allows for nondiscrete frequencies, wave-packet effects can be studied directly using LEEs. Finally, LEEs fully account for mean-flow divergence effects.

The governing equations are obtained in Sec. II via linearizing around the mean flow, which is assumed to be given by some other means (Sec. III). As pointed out in Sec. IV, a high-order numerical scheme must be employed to avoid dissipation and dispersion errors in the solution. The main difficulty with LEEs is the boundary treatment. Because the computational domain is finite, spurious modes can be introduced at the boundaries that could render the computed solution completely useless. As such, this work emphasizes proper boundary treatments, which are discussed in Sec. V. Results are given in Sec. VI for two types of inflow disturbances: a single frequency described by the linear instability wave or one that is random in time. This is followed by the Conclusions in Sec. VII.

II. LEEs

The LEEs are derived from the full Navier–Stokes equations by neglecting viscosity, and linearizing about a given mean flow $\bar{\rho}$, U, V, W, and E. Here, $\bar{\rho}$ is the mean density; U, V, and W are the mean velocities in the axial, radial, and azimuthal directions, respectively; and E is the mean total energy per unit volume. Similarly, ρ' is the perturbation density; $(\rho u)'$, $(\rho v)'$, and $(\rho w)'$ are the perturbation momentums in the axial, radial, and azimuthal directions, respectively; and e' is the perturbation total energy per unit volume. The LEEs then may be written in cylindrical coordinates as

$$(\tilde{Q})_t + (\tilde{F})_x + (1/r)(r\tilde{G})_r + (1/r)(\tilde{H})_\theta = (1/r)(\tilde{S}) \quad (1)$$

where

$$\tilde{Q} = \begin{Bmatrix} \hat{\rho} \\ \hat{u} \\ \hat{v} \\ \hat{w} \\ \hat{e} \end{Bmatrix} = \begin{Bmatrix} \rho' \\ (\rho u)' \\ (\rho v)' \\ (\rho w)' \\ e' \end{Bmatrix} \quad (2)$$

Presented as Paper 95-0505 at the AIAA 33rd Aerospace Sciences Meeting and Exhibit, Reno, NV, Jan. 9–12, 1995, and as Paper 96-0752 at the AIAA 34th Aerospace Sciences Meeting and Exhibit, Reno, NV, Jan. 15–18, 1996; received Dec. 16, 1996; revision received Aug. 4, 1997; accepted for publication Aug. 7, 1997.

*Professor, Technical Leader of Computational Aeroacoustics Group, Institute for Computational Mechanics in Propulsion.
†Senior Research Associate, Institute for Computational Mechanics in Propulsion. Member AIAA.
‡Senior Research Associate, Institute for Computational Mechanics in Propulsion. Senior Member AIAA.
§Acting Deputy Chief, Turbomachinery and Propulsion Systems Division. Fellow AIAA.

$$\tilde{F} = \begin{Bmatrix} \hat{u} \\ -\hat{\rho}U^2 + 2\hat{u}U + p' \\ -\hat{\rho}UV + \hat{v}U + \hat{u}V \\ -\hat{\rho}UW + \hat{w}U + \hat{u}W \\ U(p' + \hat{e}) + (\hat{u} - \hat{\rho}U)\left(\dfrac{P+E}{\bar{\rho}}\right) \end{Bmatrix} \tag{3}$$

$$\tilde{G} = \begin{Bmatrix} \hat{v} \\ -\hat{\rho}UV + \hat{v}U + \hat{u}V \\ -\hat{\rho}V^2 + 2\hat{v}V + p' \\ -\hat{\rho}VW + \hat{w}V + \hat{v}W \\ V(p' + \hat{e}) + (\hat{v} - \hat{\rho}V)\left(\dfrac{P+E}{\bar{\rho}}\right) \end{Bmatrix} \tag{4}$$

$$\tilde{H} = \begin{Bmatrix} \hat{w} \\ -\hat{\rho}UW + \hat{w}U + \hat{u}W \\ -\hat{\rho}VW + \hat{w}V + \hat{v}W \\ -\hat{\rho}W^2 + 2\hat{w}W + p' \\ W(p' + \hat{e}) + (\hat{w} - \hat{\rho}W)\left(\dfrac{P+E}{\bar{\rho}}\right) \end{Bmatrix} \tag{5}$$

and

$$\tilde{S} = \begin{Bmatrix} 0 \\ 0 \\ -\hat{\rho}W^2 + 2\hat{w}W + p' \\ -\hat{\rho}VW + \hat{w}V + \hat{v}W \\ 0 \end{Bmatrix} \tag{6}$$

Here, P and p' are the mean and perturbation pressures

$$P = (\gamma - 1)\bar{\rho}\left[E - \tfrac{1}{2}(U^2 + V^2 + W^2)\right] \tag{7}$$

$$p' = (\gamma - 1)\left[\hat{e} - (\hat{u}U + \hat{v}V + \hat{w}W) + \tfrac{1}{2}\hat{\rho}(U^2 + V^2 + W^2)\right] \tag{8}$$

Velocities are normalized by the reference jet exit centerline velocity U_e, time by D/U_e, density by the jet exit centerline value ρ_e, and pressure by $\rho_e U_e^2$.

III. Mean Flow

The mean flow is assumed to be given by another method (experimental, analytical, empirical, or by Reynolds-averaged equations). The mean flow used here is the analytical fit of the experimental results of Troutt and McLaughlin[18] for a supersonic ($M_e = 2.1$) jet. This analytical fit was proposed by Tam and Burton[13] to fit the measured profile of the mean-flow axial velocity in the three streamwise regimes of a supersonic jet: potential core, transitional, and fully developed. This profile was shown to describe well the experimentally measured profile. For details of the profile, see Refs. 13 and 18.

IV. Numerical Details

In computational aeroacoustics (CAA), the aim is to obtain an accurate prediction of the unsteady fluctuations representing the sound source and/or the acoustic field. Special attention, therefore, must be placed on how the numerical algorithm and boundary conditions can handle wave-type solutions. Sankar et al.[19] and Scott et al.[20] have evaluated several schemes for use in CAA. The performance of the 2-4 MacCormack-type scheme was considered satisfactory because of its accuracy, speed, and simplicity. This 2-4 scheme is an extension of the classical second-order-accurate MacCormack scheme[21] to fourth-order accuracy in space and second-order accuracy in time.[22]

For the axisymmetric case, the solver is split into radial and axial operators and applied in a symmetric way to avoid numerical biasing of the solution:

$$\tilde{Q}^{n+2} = L_x L_r L_r L_x \tilde{Q}^n \tag{9}$$

Each operator consists of a predictor step and a corrector step; each step uses a one-sided difference. For the streamwise direction, it takes the following form.

Predictor:

$$\tilde{Q}_i^{n+\frac{1}{2}} = \tilde{Q}_i^n + \frac{\Delta t}{6\Delta x}(7\tilde{F}_i - 8\tilde{F}_{i-1} + \tilde{F}_{i-2})^n \tag{10}$$

Corrector:

$$\tilde{Q}_i^{n+1} = \frac{1}{2}\left[\tilde{Q}_i^n + \tilde{Q}_i^{n+\frac{1}{2}} - \frac{\Delta t}{6\Delta x}(7\tilde{F}_i - 8\tilde{F}_{i+1} + \tilde{F}_{i+2})^{n+\frac{1}{2}}\right] \tag{11}$$

and likewise for the other direction. The order of the sweep directions is reversed between operators to avoid numerical biasing. At the computational boundaries, the flux quantities are needed to perform the spatial derivatives; these are obtained using third-order extrapolations based on data from the interior of the domain:

$$F_{i+1} = 4F_i - 6F_{i-1} + 4F_{i-2} - F_{i-3} \tag{12}$$

To ensure grid independence and accuracy of the results presented herein, various levels of grid refinement were considered. It was found that at least 25 points per wavelength are required to obtain a grid-independent solution. The grid used herein is such that this constraint on the minimum number of points per wavelength is satisfied for the shortest wavelength calculated here.

Because grid stretching reduces the solution accuracy of the 2-4 scheme, a uniform grid is used wherever possible. The physics of the problem do not require stretching in the axial direction; thus, 196 evenly spaced points are used in a domain extending from $2.5 < x/D < 35$. In the radial direction, more grid points must be concentrated where the mean flow gradient is maximum to resolve the physics involved in the development of the disturbance mode. In the radial direction, the grid begins just above the centerline ($r/D = 0.005$) and extends to $r/D = 16$, with a total of 381 points. The grid is uniform from the centerline to $r/D = 0.5$ with a spacing of $\Delta r/D = 0.005$. At this point, the grid is stretched geometrically by a factor of 1.01 until the radial spacing is equal to the axial spacing. At this point, the grid spacing is uniform to the outer radial boundary.

A large number of grid points is needed to resolve steep mean-velocity gradients, and the solution could be unstable because of a lack of damping effects. In real jets, large mean-velocity gradients correspond to large amplification rates of the disturbances, but this is dampened by nonlinear and viscous effects lacking in the present formulation. To avoid imposing artificial dissipation, which could hide problems resulting from boundary treatments, the computation is started from an axial distance of $x/D = 2.5$ downstream of the nozzle exit.

V. Boundary Treatments

Special attention is given to the boundary treatment in order to avoid nonphysical oscillations, which can render the computed unsteady solution unacceptable. To provide guidance for this problem, several boundary treatments were first considered for a model problem.[23] The boundary treatments discussed in the subsections below were found to be stable, essentially nonreflecting, and suitable for the present jet noise computations.

There are four boundary conditions used in the computation, as shown in Fig. 1: inflow, radiation, centerline, and outflow. These boundary treatments are described in Secs. V.A–V.D, respectively.

A. Inflow Boundary Condition

In the fluid disturbance region ($x/D = x_{\min}, r/D < 2$), input disturbances are introduced into the flowfield (Sec. VI). To accomplish this, the time derivatives of the disturbance are added to the computed flow variables at each time step:

$$(\tilde{Q}_t)_{\text{boundary}} = (\tilde{Q}_t)_{\text{computed}} + (\tilde{Q}_t)_{\text{disturbance}} \tag{13}$$

1. *Characteristic Inflow Boundary Condition*

To determine $(\tilde{Q}_t)_{\text{computed}}$, a one-dimensional characteristic inflow boundary condition following Thompson's analysis is used.[24,25] In

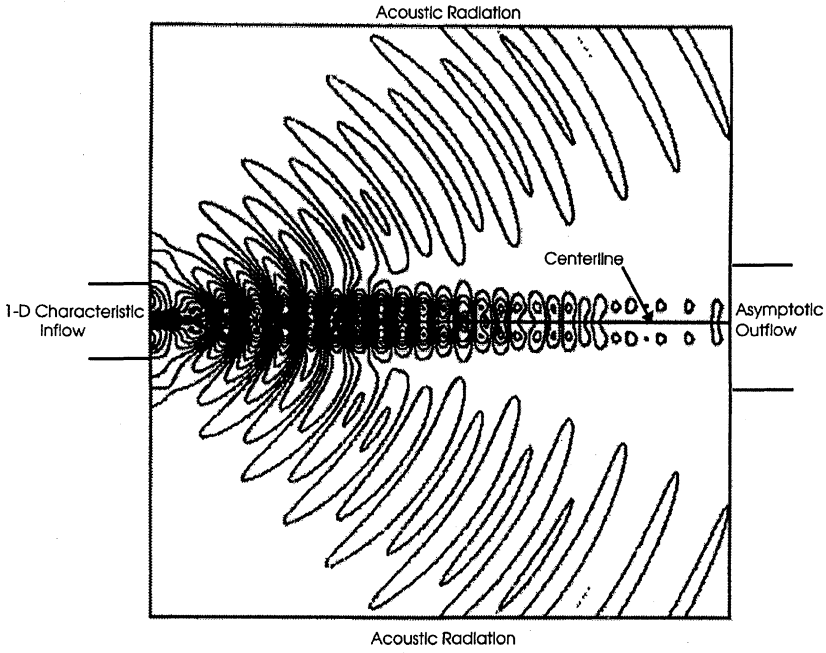

Fig. 1 Pressure disturbance field and boundary conditions.

this analysis, the time derivative at the inflow boundary is decomposed into its component parts:

$$\tilde{Q}_t = \tilde{Q}_t|_{\text{axial}} + \tilde{Q}_t|_{\text{radial}} + \tilde{Q}_t|_{\text{azimuthal}} + \tilde{Q}_t|_{\text{source}} \tag{14}$$

Here,

$$\tilde{Q}_t|_{\text{axial}} = \begin{Bmatrix} (\rho')_t|_{\text{axial}} \\ (\rho u)'_t|_{\text{axial}} \\ (\rho v)'_t|_{\text{axial}} \\ (\rho w)'_t|_{\text{axial}} \\ (e')_t|_{\text{axial}} \end{Bmatrix} = \begin{Bmatrix} \hat{u} \\ -\hat{\rho}U^2 + 2\hat{u}U + p' \\ -\hat{\rho}UV + \hat{v}U + \hat{u}V \\ -\hat{\rho}UW + \hat{w}U + \hat{u}W \\ U(p' + \hat{e}) + (\hat{u} - \hat{\rho}U)\left(\dfrac{P+E}{\bar{\rho}}\right) \end{Bmatrix}_x \tag{15}$$

$$(\rho')_t|_{\text{axial}} = \frac{\frac{1}{2}(R_1 + R_5) - R_2}{\bar{c}^2}, \qquad (u')_t|_{\text{axial}} = \frac{(R_1 - R_5)}{2\bar{\rho}\bar{c}}$$

$$(v')_t|_{\text{axial}} = R_3, \qquad (w')_t|_{\text{axial}} = R_4 \tag{17}$$

$$(p')_t|_{\text{axial}} = \tfrac{1}{2}(R_1 + R_5)$$

For a supersonic inflow, all characteristics are incoming, and all are set to zero. To prevent spurious oscillations, the amplitude of the outgoing characteristic is set smoothly to zero near the sonic line.

Once the primitive perturbation variables are determined, the conservative perturbation variables can be updated using

$$\begin{Bmatrix} (\rho')_t \\ (\rho u)'_t \\ (\rho v)'_t \\ (\rho w)'_t \\ (e')_t \end{Bmatrix} = \begin{Bmatrix} (\rho')_t \\ \bar{\rho}(u')_t + U(\rho')_t \\ \bar{\rho}(v')_t + V(\rho')_t \\ \bar{\rho}(w')_t + W(\rho')_t \\ \dfrac{(p')_t}{\gamma - 1} + [U(\rho u)'_t + V(\rho v)'_t + W(\rho w)'_t] - \dfrac{1}{2}(U^2 + V^2 + W^2)(\rho')_t \end{Bmatrix} \tag{18}$$

Next, the axial operator is decomposed into five one-dimensional characteristics. At a subsonic inflow boundary, four of these characteristics are incoming and are set to zero for a nonreflecting boundary condition: The fifth characteristic is outgoing and is computed from the flow solution

$$R_1 = (p')_t|_{\text{axial}} + \bar{\rho}\bar{c}(u')_t|_{\text{axial}} = 0$$

$$R_2 = (p')_t|_{\text{axial}} - \bar{c}^2(\rho')_t|_{\text{axial}} = 0$$

$$R_3 = (v')_t|_{\text{axial}} = 0, \qquad R_4 = (w')_t|_{\text{axial}} = 0 \tag{16}$$

$$R_5 = (p')_t|_{\text{axial}} - \bar{\rho}\bar{c}(u')_t|_{\text{axial}} = [(p')_t|_{\text{axial}} - \bar{\rho}\bar{c}(u')_t|_{\text{axial}}]_{\text{computed}}$$

The five characteristic equations then are solved together to obtain the time derivatives of the variables at the inflow boundary:

Because of the specified mean velocity at the fluid inflow boundary, the Thompson inflow boundary condition exhibits a problem in which some disturbances are convected in a radial direction and remain on the boundary for the rest of the computation. To alleviate this, the mean radial velocity is set to zero on the inflow boundary, and is raised smoothly to the proper value by $x/D = 3.0$.

2. *Input Disturbance*

Two types of input disturbances are used. The first is an instability-wave disturbance, which is assumed to be in the following form:

$$\begin{Bmatrix} \rho' \\ u' \\ v' \\ w' \\ p' \end{Bmatrix} = Re \begin{Bmatrix} \breve{\rho}(r) \\ \breve{u}(r) \\ \breve{v}(r) \\ 0 \\ \breve{p}(r) \end{Bmatrix} e^{i(\alpha x - \omega t)} \tag{19}$$

The radial distribution of these complex eigenfunctions is obtained by solving the Orr–Sommerfeld equation for the given frequency ω. This solution extends to $r/D = 1$, and a curve is fitted to smoothly set the disturbance to zero by $r/D = 2$.

The second type of input disturbance is a random excitation, of the form

$$(Q_t)_{\text{disturbance}} = A_{\text{random}}(t) \exp\left[-\ell_n(2) \cdot \left(\frac{r-h}{b}\right)^2\right] \tag{20}$$

Here, $b = 0.1$, $h = 0.78361$, and A_{random} ranges from $-1.0e$-3 to $1.0e$-3. The excitation is random only in time, not in space. A random-number generator is used to determine A_{random}; each conserved variable is assigned a different random value of A_{random} at each time step.

The random disturbance is limited to a range of frequencies $0.025 < Sr < 1.6$. The lower limit is imposed to aid in acquiring results, and the upper limit is imposed because of the few points per wavelength at the higher frequencies.

To impose these restrictions, a random distribution of points is taken over a nondimensional time of 80 (a period of $Sr = 0.025$). Enough points are taken to resolve a maximum frequency of $Sr = 1.6$. To determine the excitation level at each time level, an Akima spline is used to interpolate between the random points. The result is taken to be one period of excitation; at the end of each period, the cycle of excitation is repeated.

B. Radiation Boundary Condition

The radiation boundary condition is applied to three regions, as shown in Fig. 1:

$$\begin{aligned} x/D &= x_{\min}, & r/D &> 2 \\ x_{\min} < x/D &< x_{\max}, & r/D &= r_{\max} \\ x/D &= x_{\max}, & M_{\text{exit}} &< 0.01 \end{aligned} \tag{21}$$

In these regions, the conventional acoustic radiation boundary condition is used, namely

$$q_t = -V(\theta)[(x/R)q_x + (r/R)q_r + (1/R)q] \tag{22}$$

where

$$q = \begin{Bmatrix} \rho' \\ u' \\ v' \\ p' \end{Bmatrix}, \qquad R = \sqrt{x^2 + r^2}$$
$$V(\theta) = \bar{c}\left\{(x/R)M + \sqrt{1 - [(r/R)M]^2}\right\} \tag{23}$$

and M is the local Mach number. The spatial derivatives that appear in Eq. (23) are evaluated in a manner identical to that for the inner flow derivatives. Equation (18) is used to transform the time derivatives of the primitive variables to the conserved variables.

C. Centerline Boundary Condition

In this code, the centerline boundary is represented with a point at the centerline, and a ghost point is reflected across the centerline in the radial direction. In a fully three-dimensional calculation, the centerline treatment for a three-dimensional problem is not straightforward, and has been addressed by Shih et al.[26] However, for an axisymmetric calculation, the boundary condition at $r = 0$ becomes straightforward:

$$v = 0 \tag{24}$$

and

$$\frac{\partial}{\partial r}\begin{Bmatrix} \rho' \\ u' \\ p' \end{Bmatrix} = 0 \tag{25}$$

D. Outflow Boundary Condition

The outflow boundary condition is a stumbling block in the computation of high-speed jets, because it must allow outgoing acoustic, vorticity, and entropy waves to travel in a nonuniform mean flow through the boundary without generating spurious reflections.

The outflow boundary treatment is based on the asymptotic analysis of the linearized equations as given by Tam and Webb.[27] The pressure condition is the same as that obtained by Bayliss and Turkel,[28] Engquist and Majda,[29] and Hagstrom and Hariharan,[30] namely

$$(p')_t|_{\text{BC}} = -V(\theta)[(x/R)p'_x + (r/R)p'_r + (1/R)p'] \tag{26}$$

As in the acoustic radiation boundary condition,

$$R = \sqrt{x^2 + r^2}$$
$$V(\theta) = \bar{c}\left\{(x/R)M + \sqrt{1 - [(r/R)M]^2}\right\} \tag{27}$$

However, for updating the rest of the primitive variables, Tam and Webb[27] have shown that the momentum and continuity equations should be used to account for the presence of entropy and vorticity waves at the outflow boundary. Thus, the perturbation density and momentum equations at the boundary are unchanged, but the energy equation is replaced with

$$(e')_t|_{\text{BC}} = \frac{(p')_t|_{\text{BC}}}{\gamma - 1} + [U(\rho u)'_t|_{\text{inner}} + V(\rho v)'_t|_{\text{inner}} + W(\rho w)'_t|_{\text{inner}}] - \frac{1}{2}(U^2 + V^2 + W^2)(\rho')_t|_{\text{inner}} \tag{28}$$

The spatial differencing used in the inner code is employed to evaluate the derivatives that appear in Eq. (24).

For the outflow boundary at large radius and a local Mach number of less than 0.01, the outflow boundary condition is replaced with the radiation boundary condition.

Note that the Tam and Webb[27] outflow boundary condition is formulated with an assumption that the mean flow is uniform, which is not true for the jet outflow boundary. However, the results given by this boundary condition are quite good, with very little reflection.

VI. Results

Results are presented in Secs. VI.A–VI.C for the axisymmetric disturbance flow and acoustic field of an unheated supersonic jet ($M_{\text{exit}} = 2.1$) with a uniform stagnation temperature of 270 K. We split the discussion of the results into three subsections. In Sec. VI.A, the objective is to examine how clean the numerical solution is. In Sec. VI.B, we examine the results for instability-wave radiation in comparison with the theoretical analysis of Tam and Burton.[13] This is followed in Sec. VI.C by a discussion of the applicability of the present results to real jets.

A. Accuracy of the Solution

Dispersion and dissipation errors in the interior scheme as well as reflections from the boundaries can lead to spurious modes that contaminate the solution. As such, the question that we attempt to address in this section is how clean the numerical solution is.

In Fig. 1 we show the global disturbance pressure field, and in Fig. 2 we show the global fields of the radial and axial components of the velocity and its dilation. In the near field, we note the oscillatory nature of the sound source. The sound source radiates sound that seems to peak at an angle influenced by the streamwise position where the disturbance reaches a maximum. As Figs. 1 and 2 indicate, the solution exhibits the wave nature of the acoustic fields with little or no dispersion. As for boundary reflections, these figures show the entire computational domain, i.e., there are no exit zones or sponge layers to protect the interior domain from reflections. Thus, the exit boundary treatment used here has the advantage of not wasting some computational domain as a buffer region. There are hardly any reflections from the boundaries. Furthermore, we intentionally decided not to add any artificial dissipation to the scheme (which could damp spurious modes) to provide a critical test of the present boundary treatments.

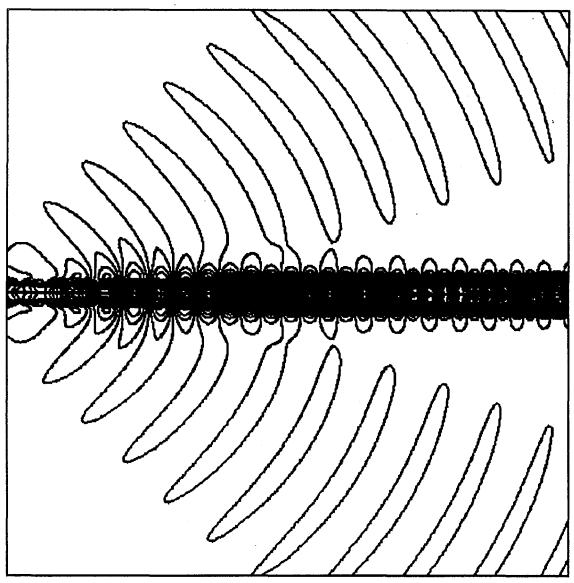

Fig. 2a Axial velocity-disturbance field.

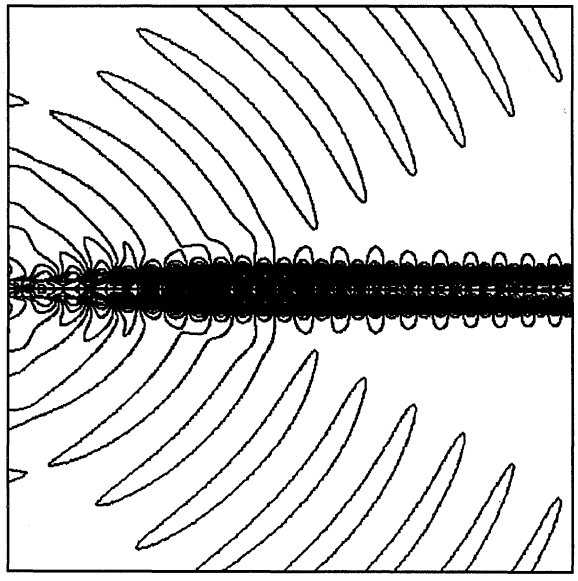

Fig. 2b Radial velocity-disturbance field.

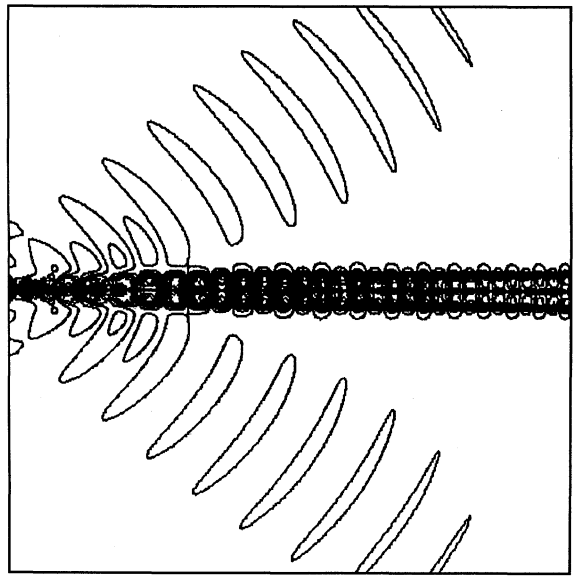

Fig. 2c Dilation of disturbance velocity.

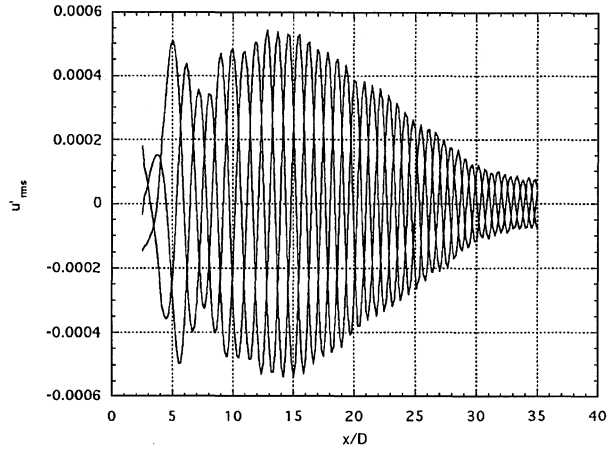

Fig. 3 Axial velocity-disturbance along the $r/D = 0.5$ line.

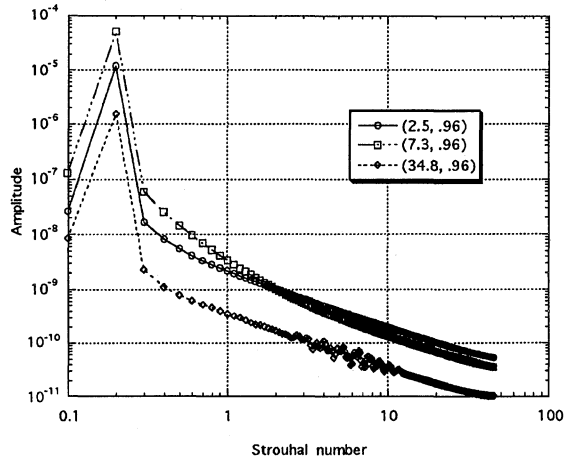

Fig. 4 Pressure spectra at various locations.

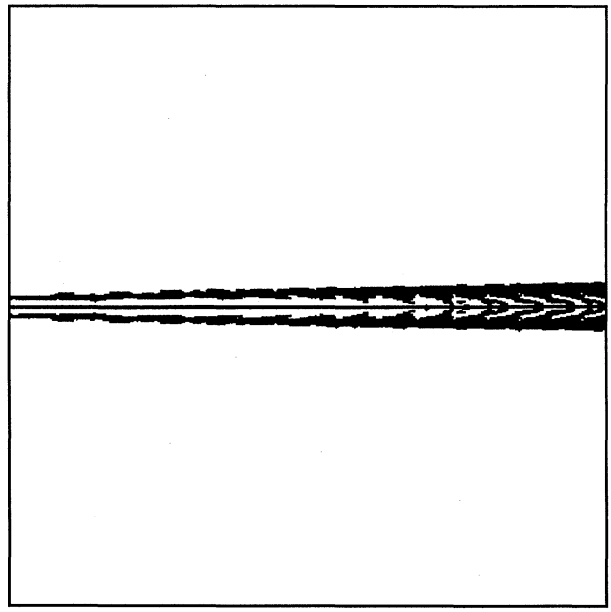

Fig. 5 Disturbance vorticity.

In Figs. 3–6, we attempt to present further criteria for examining the accuracy of the solution. In Fig. 3, we show the oscillatory distribution of the axial velocity disturbance along the $r/D = 0.5$ line at several times. The wave nature of the sound source is apparent even near the outflow boundary. Further, we examine the spectra in Fig. 4. These spectra are calculated by taking the time history of the data at a point over two cycles of oscillation and performing a fast Fourier transform. This is a linear code with a single frequency inflow disturbance; thus, if other frequency modes exist in the solution, they

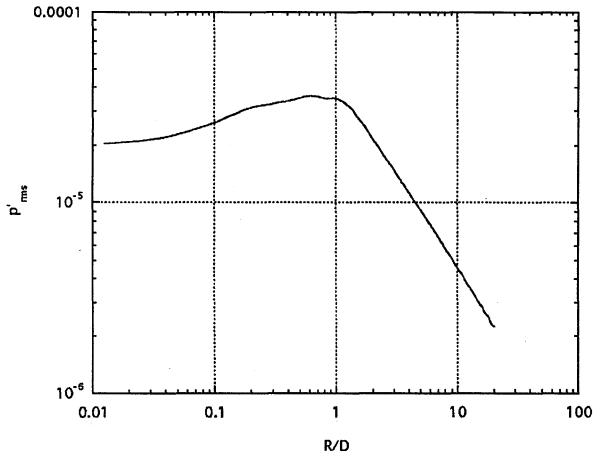

Fig. 6 Radial decay of pressure disturbance in the far field.

would have to be nonphysical and due to numerical errors. Figure 4 shows the spectra at different locations in the domain. Clearly, all nonfundamental modes are at least two orders of magnitude lower than the imposed one. This indicates that the solution is practically free from spurious modes.

We move in Figs. 5 and 6 to examining how clean the computed acoustic field is. The acoustic field must be irrotational and decaying as a function of $1/R$. Indeed, Fig. 5 shows that the vorticity field is restricted to the shear-layer area and is zero in the outer acoustic field. Furthermore, Fig. 6 shows that the rms pressure decays as a function of $1/R$ in the outer field, as an acoustic field should behave. From the results of Figs. 5 and 6, one can conclude that the computed outer field is indeed an acoustic one.

B. Validation Against Theoretical Results for Instability Waves

As pointed out earlier, several researchers believe that instability waves can provide a reasonable model for prediction of supersonic jet noise. Given that LEEs are more general than the instability-wave equations, we attempt herein to address the question of whether the present code can be used for prediction of instability-wave noise.

Tam and Burton[13] used asymptotic methods to study sound radiated by an instability wave in a supersonic jet. The Rayleigh equation is used to describe the sound field in the near field, and then a matched asymptotic expansion is used to obtain the corresponding sound field radiated by a single instability wave. Comparisons are made here between the theoretical results and the numerical one for a Strouhal number $Sr = fD/U_e = 0.2$, where f is the frequency in hertz. The mean flow in both cases is that of Sec. III.

We show in Fig. 7 the numerically obtained maximum values of the pressure oscillations. The lobe shape with lateral peak is evident in the solution, which is in qualitative agreement with the theoretical results. For a quantitative comparison, we show in Fig. 8 the contours of the sound pressure levels superposed on the results of Tam and Burton. Since the magnitude of the input disturbance used by Tam and Burton was not known, a single data point in the domain was matched with their results. Once the magnitude is determined, this is used in all of the results given. The end result shows the very good agreement between the two methods for the sound radiation pattern and directivity.

C. Effect of Input Disturbances

What we have shown so far is that the present LEE approach can produce a clean solution and can be used successfully for prediction of sound attributed to instability waves. Because instability waves are believed to be a reasonable representation of the sound source, and because LEEs are more general than the instability-wave equations, one is tempted to address the question of how far LEEs can go in representing noise produced by real supersonic jets.

At the outset we recall that, because nonlinearity is missing in LEEs, the present authors believe that only large-scale simulations can provide a complete picture of jet noise. Yet, LEEs still can be a useful tool in predicting jet noise. For one thing, they can be used for extending a nonlinear near-field solution, e.g., LES or DNS,[31,32]

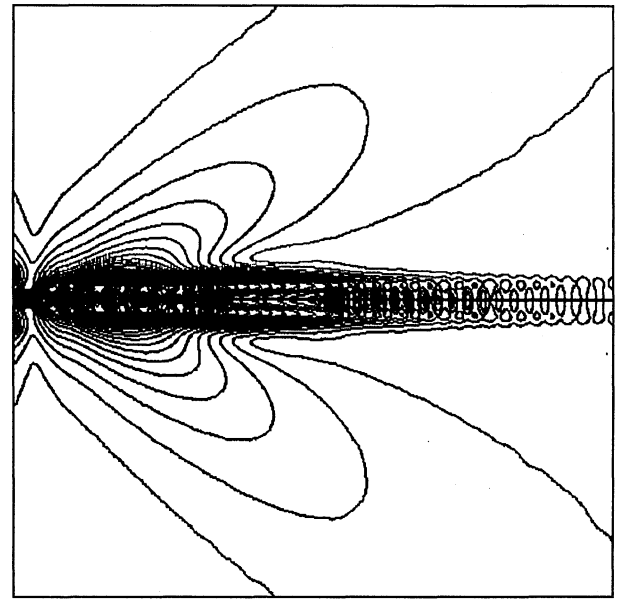

Fig. 7 Maximum values of pressure disturbance.

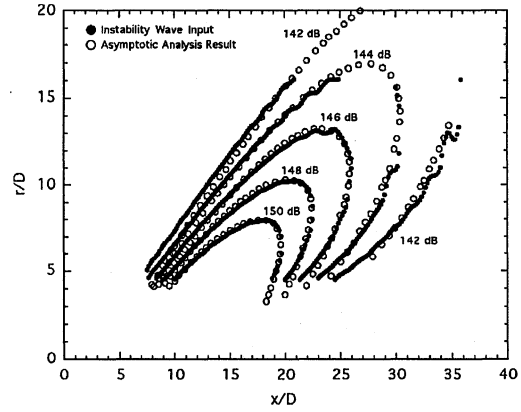

Fig. 8 Sound pressure-level contours of the present calculation compared with results of asymptotic analysis.

to obtain the far-field solution, which is linear. Further investigation of this issue is made by Shih et al.[33] Then, the remaining question is how well LEEs can approximate the near field of real supersonic jets. Among other parameters, the nature of the disturbances exiting from the nozzle could play a key role in addressing this question. The flow inside the nozzle preceding the jet determines the inflow to the jet and therefore the radiated sound. Mean parameters (mean flow shape, temperature, Mach number, etc.) usually are specified in the experiment. The difficulty is with the nature of the disturbance issuing from the nozzle, which is rarely given in the experimental results. Dong and Mankbadi[34] are beginning to address this difficulty by computing the unsteady flow inside the nozzle to obtain the jet's inflow disturbances (spectra, radial shapes, intensity, randomness, etc.).

Lacking, at present, a definite description of the nozzle exit unsteady flow, one has to make assumptions. Maestrello et al.[35] and Bayliss and Maestrello[36] attempted to account for the effect of nozzle flow on the jet noise by considering the interaction of a sound pulse with the jet flow. Another approach is the instability-wave mode discussed earlier. In real jets, however, the inflow disturbances are mostly random, composed of various frequencies. Therefore, we present results in which the inflow disturbances are taken to be semi-random in time, as explained after Eq. (20). Computed results are compared with the experimental results of Troutt and McLaughlin,[18] who measured sound radiated by a Mach 2.1 jet. They attempted to excite it with a single, axisymmetric disturbance at $Sr = 0.2$. However, other axisymmetrical and three-dimensional modes were present, and the initial excitation level was not well defined.

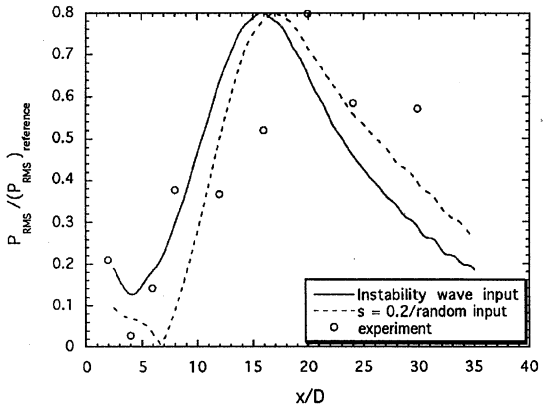

Fig. 9 RMS pressure disturbance along the $r/D = 8$ line.

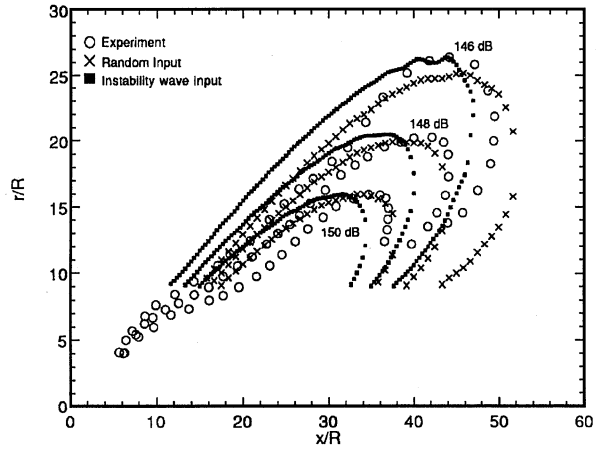

Fig. 10 Comparison of sound pressure-level contours for instability wave and random input with experiment.

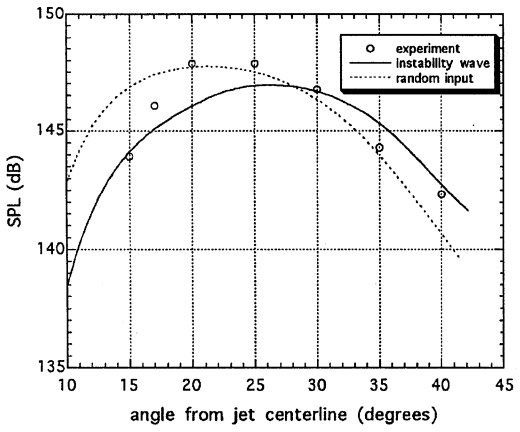

Fig. 11 Sound directivity at $R/D = 24$.

In Fig. 9, we compare the calculated rms of the pressure fluctuations along the $r/D = 8.0$ line with experimental results. The initial disturbance level is roughly the same for both computation and experiment, and the maximum value of the graphs is matched. The $Sr = 0.2$ component of the random input was filtered out using fast Fourier transforms to compare it with the experimental measurements as well as with the earlier numerical results for an instability-wave input disturbance. There is a slight shift in the numerical results of the instability wave as compared to that of the same frequency component of the random disturbances. This is attributed to the different receptivity of the two cases. As pointed out by Tam and Burton,[18] the experimentally measured sound source was composed of axisymmetric and helical modes, with the latter more dominant than the former. The numerical results shown here are only for the axisymmetric mode. As such, only qualitative agreement between the numerical results and the experimental measurements are obtained.

In Fig. 10, the contour plots of the sound radiation at $Sr = 0.2$ for the random input and instability-wave input are compared with experiment. The results are in good qualitative agreement with experiment, with the case of random input disturbances closer to the experiment than the instability-wave calculations.

The angular directivity of the sound pressure level is shown in Fig. 11. This is calculated at a radius of $R/D = 24$ from the nozzle exit centerline. The peak noise occurs at 21, 22, and 26 deg for calculated random disturbances, experimental results, and instability-wave inputs, respectively. Evidently, the random input disturbance is closer to the real jet results than an instability-wave model. However, the calculated results still slightly differ from measurements because of the reasons discussed previously.

VII. Conclusions

A computationally inexpensive approach based on the LEEs is introduced for the analysis of supersonic jet noise. A high-order numerical scheme is adopted to reduce dissipation and dispersion error. The main difficulty of using the LEEs for sound prediction is the spurious modes that could be generated at the computational boundaries. The boundary treatments used here are shown to produce a stable solution free from artificial boundary reflections or spurious modes while preserving the wavy nature of the solution. As such, these boundary treatments are most suitable for jet noise computation.

Comparisons between experiment and theory indicate that the present tool can be used for accurate prediction of sound propagation in the linear domain surrounding the sound generation domain. Thus, the approach can be used to extend nonlinear, near-field computation, e.g., LES or DNS, to obtain the radiated far-field sound with considerable reduction in computation time compared to direct LES or DNS computation. Unlike the classical Kirchhoff method for extension of the near field to the far field, LEEs account for refraction effects caused by nonuniform mean flow. Furthermore, the present approach avoids matching problems associated with the asymptotic-expansion approach to noise prediction.

Two types of unsteady inflow disturbances were studied to clarify their effect on the radiated sound. In the first, the disturbances were taken to be single-frequency instability waves. In the second, the disturbances were assumed to be random in time. It was shown that the radiated sound field is dependent on the nature of the input disturbance. Time-random inflow disturbances seem to produce an acoustic field that resembles the experimental observations more than that of the linear instability modes.

Can LEEs predict the sound generation as well as the sound propagation? The linear instability-wave equations are known to produce results that resemble radiation of supersonic jets. Thus, it is not surprising that LEE, which is more general than the linear instability-wave equations, produces results consistent with observations, as shown herein. However, in other cases, such as low-Mach-number jets, nonlinearity may be important but cannot be captured by the present approach. As such, although LEEs can accurately predict the sound propagation, they should be treated as an approximate but fast tool for prediction of the sound source.

References

[1]Mankbadi, R. R., Hayder, M. E., and Povinelli, L. A., "Structure of Supersonic Jet Flow and Its Radiated Sound," *AIAA Journal*, Vol. 32, No. 5, 1994, pp. 897–906.

[2]Mankbadi, R. R., Shih, S.-H., Hixon, R., and Povinelli, L. A., "Direct Computation of Acoustic and Flow Field of a Supersonic Jet Using Large-Eddy Simulation," AIAA Paper 95-0680, Jan. 1995.

[3]Seiner, J. M., McLaughlin, D. K., and Liu, C. H., "Supersonic Jet Noise Generated by Large-Scale Instabilities," NASA TP-2072, Sept. 1982.

[4]Zaman, K. B. M. Q., "Flow Field and Near and Far Sound Field of a Subsonic Jet," *Journal of Sound and Vibration*, Vol. 106, No. 1, 1986, pp. 1–6.

[5]Mankbadi, R. R., and Liu, J. T. C., "Sound Generated Aerodynamically Revisited: Large-Scale Structures in a Turbulent Jet as a Source of Sound," *Philosophical Transactions of the Royal Society of London, Series A: Mathematical and Physical Sciences*, Vol. 311, No. 1516, 1984, pp. 183–217.

[6]Mankbadi, R. R., "The Self-Noise from Ordered Structures in a Low Mach Number Jet," *Journal of Applied Mechanics*, Vol. 57, March 1990, pp. 241–246.

[7]Tam, C. K. W., "Jet Noise Generated by Large-Scale Coherent Motion," *Aeroacoustics of Flight Vehicles: Theory and Practice, Vol. 1: Noise Source*, edited by H. H. Hubbard, NASA RP-1258, 1991, Chap. 6.

[8]Mankbadi, R. R., *Transition, Turbulence, and Noise*, Kluwer Academic, Norwell, MA, 1994, Chap. 6.

[9]Laufer, J., and Yen, T. C., "Noise Generation by a Low Mach Number Jet," *Journal of Fluid Mechanics*, Vol. 62, 1983, pp. 437–464.

[10]Liu, J. T. C., "Developing Large-Scale Wavelike Eddies and the Near Jet Noise Field," *Journal of Fluid Mechanics*, Vol. 62, 1974, pp. 437–461.

[11]Morris, P., "A Model for the Structure of Jet Turbulence as a Source of Noise," AIAA Paper 74-1, Jan. 1974.

[12]Morris, P., and Tam, C. K. W., "On the Radiation of Sound by Instability Waves of a Compressible Axisymmetric Jet," *Mechanics of Sound Generation in Flows*, Springer–Verlag, Berlin, 1979, pp. 55–61.

[13]Tam, C. K. W., and Burton, D. E., "Sound Generated by Instability Waves of Supersonic Flows, Part 2: Axisymmetric Jets," *Journal of Fluid Mechanics*, Vol. 138, 1984, pp. 273–295.

[14]McLaughlin, D. K., Seiner, J. M., and Liu, C. H., "On Noise Generated by Large Scale Instabilities in Supersonic Jets," AIAA Paper 80-0964, Jan. 1980.

[15]Crighton, D. G., and Huerre, P., "Shear Layer Pressure Fluctuations and Superdirective Acoustic Sources," *Journal of Fluid Mechanics*, Vol. 220, 1990, pp. 355–368.

[16]Seiner, J. M., Bhat, T. R., and Ponton, M. K., "Mach Wave Emission from High-Temperature Supersonic Jet," AIAA Paper 93-0734, Jan. 1993.

[17]Tam, C. K. W., "Supersonic Jet Noise," *Annual Review of Fluid Mechanics*, Vol. 27, 1995, p. 17.

[18]Troutt, T. R., and McLaughlin, D. K., "Experiments on the Flow and Acoustic Properties of a Moderate Reynolds Number Supersonic Jet," *Journal of Fluid Mechanics*, Vol. 116, 1982, pp. 123–156.

[19]Sankar, L. N., Reddy, N. N., and Hariharan, N., "A Comparative Study of Numerical Schemes for Aero-Acoustic Applications," *Computational Aero- and Hydro-Acoustics*, Vol. 147, Fluid Engineering Div., American Society of Mechanical Engineers, New York, 1993, pp. 35–40.

[20]Scott, J. N., Hariharan, S. I., and Mankbadi, R. R., "Evaluation of Numerical Schemes for the Analysis of Sound Generated by Blade-Gust Interaction," *Proceedings of the ICASE/LaRC Workshop on Benchmark Problems for CAA* (Hampton, VA), NASA CP-3300, May 1995.

[21]MacCormack, R. W., "The Effect of Viscosity in Hypervelocity Impact Cratering," AIAA Paper 69-354, 1969.

[22]Gottleib, D., and Turkel, E., "Dissipative Two-Four Method for Time Dependent Problems," *Mathematics of Computation*, Vol. 30, No. 136, 1976, pp. 703–723.

[23]Hixon, R., Shih, S.-H., and Mankbadi, R. R., "Evaluation of Boundary Conditions for Computational Aeroacoustics," *AIAA Journal*, Vol. 33, No. 11, 1995, pp. 2006–2012.

[24]Thompson, K. W., "Time-Dependent Boundary Conditions for Hyperbolic Systems," *Journal of Computational Physics*, Vol. 68, Jan. 1987, pp. 1–24.

[25]Thompson, K. W., "Time-Dependent Boundary Conditions for Hyperbolic Systems II," *Journal of Computational Physics*, Vol. 89, Aug. 1990, pp. 439–461.

[26]Shih, S.-H., Hixon, R., and Mankbadi, R. R., "Three-Dimensional Structure in a Supersonic Jet: Behavior Near Centerline," AIAA Paper 95-0681, Jan. 1995.

[27]Tam, C. K. W., and Webb, J. C., "Dispersion-Relation-Preserving Finite Difference Schemes for Computational Acoustics," *Journal of Computational Physics*, Vol. 107, Aug. 1993, pp. 262–281.

[28]Bayliss, A., and Turkel, E., "Far Field Boundary Conditions for Compressible Flows," *Journal of Computational Physics*, Vol. 48, No. 2, 1982, pp. 182–199.

[29]Engquist, B., and Majda, A., "Radiation Boundary Conditions for Acoustic and Elastic Wave Calculations," *Communications on Pure and Applied Mathematics*, Vol. 32, No. 3, 1979, pp. 312–358.

[30]Hagstrom, T., and Hariharan, S. I., "Far Field Expansion for Anisotropic Wave Equations," *Computational Acoustics*, Vol. 2, 1990.

[31]Mitchell, B. E., Lele, S. K., and Moin, P., "Direct Computation of the Sound Generated by Subsonic and Supersonic Axisymmetric Jets," Stanford Univ., TR TF-66, Stanford, CA, 1995.

[32]Freund, J. B., Moin, P., and Lele, S. K., "Results of a Compressible Round Shear Layer Direct Simulation," AIAA Paper 97-0760, Jan. 1997.

[33]Shih, S.-H., Hixon, R., and Mankbadi, R. R., "A Zonal Approach for Prediction of Jet Noise," *Journal of Propulsion and Power* (to be published); CEAS/AIAA Paper 95-144, June 1995.

[34]Dong, T. Z., and Mankbadi, R. R., "Direct Numerical Simulations of Internal Noise Propagation and Radiation," CEAS/AIAA Paper 95-064, 1995.

[35]Maestrello, L., Bayliss, A., and Turkel, E., "On the Interaction of a Sound Pulse with the Shear Layer of an Axisymmetric Jet," *Journal of Sound and Vibration*, Vol. 74, No. 2, 1981, pp. 281–301.

[36]Bayliss, A., and Maestrello, L., "On the Interaction of a Sound Pulse with the Shear Layer of an Axisymmetric Jet II: Heated Jets," *Journal of Sound and Vibration*, Vol. 86, No. 3, 1983, pp. 395–409.

S. Glegg
Associate Editor